

Temperature-dependent Raman spectra of $\text{Bi}_2\text{Sn}_2\text{O}_7$ ceramics

R.X. Silva^a, C.W.A. Paschoal^{a,*}, R.M. Almeida^b, M. Carvalho Castro Jr.^c,
A.P. Ayala^c, Jeffrey T. Auletta^d, Michael W. Lufaso^d

^a Departamento de Física, Universidade Federal do Maranhão, Campus do Bacanga, 65080-040 São Luis, MA, Brazil

^b Departamento de Física, Universidade Federal de Minas Gerais, ICEx, 31270-901 Belo Horizonte, MG, Brazil

^c Departamento de Física, Universidade Federal do Ceará, Campus do Pici, PO Box 6030, 60455-970 Fortaleza, CE, Brazil

^d Department of Chemistry, University of North Florida, 1 UNF Drive, Jacksonville, FL 32224, USA

ARTICLE INFO

Article history:

Received 17 November 2011

Received in revised form 9 May 2012

Accepted 14 May 2012

Available online 24 May 2012

Keywords:

$\text{Bi}_2\text{Sn}_2\text{O}_7$

Pyrochlore

Raman

Ceramic

Phase transition

ABSTRACT

The $\text{Bi}_2\text{Sn}_2\text{O}_7$ pyrochlore is known to undergo a sequence of structural phase transitions with an increase in temperature. Raman spectroscopy was employed in the investigation of the temperature dependence of the active phonons in the Raman spectrum. We observed 19 broad modes at room temperature, reflecting the low symmetry of the α -phase of $\text{Bi}_2\text{Sn}_2\text{O}_7$. The modes were discussed in relation to the Raman spectra of other pyrochlore-based oxides. The temperature dependence of the phonons evidences the $\alpha \rightarrow \beta$ structural phase transition observed near 127 °C.

© 2012 Elsevier B.V. All rights reserved.

1. Introduction

Ternary metal oxides with a pyrochlore related-structure, whose chemical formula is $\text{A}_2\text{B}_2\text{X}_7$, where A is a larger cation e.g. Ca, K, Ba, Y, Ce, Pb, U, Sr, Cs, Na, Sb, Bi and Th; B is a metal cation, e.g. Nb, Ta, Ti, Sn, Fe and W; and X is an anion, e.g. O^{2-} , OH^- or F^- ; have been extensively investigated [1,2]. The great variety of site substitutions on both the A and B sites have led to an assortment of interesting physical and chemical properties, such as ferroelectricity [1–4], high and stable permittivity under a broad temperature range [5,6], oxygen fast ionic conduction, semiconductivity, superconductivity and electronic phase transitions [1,7–11] among others. These materials have also found application as catalysts [12,13], fluorescent centers [14], nuclear residue storage [15], cathodes and electrolyte for solid oxide fuel cells (SOFC) [16–19], thermal barrier coatings (TBC) [20–22], multilayer capacitors and dielectric resonators [23], gas sensors, thermistors, switch elements and resistors [24,25]. The pyrochlore of this study, $\text{Bi}_2\text{Sn}_2\text{O}_7$ (BSO), is interesting due to its catalytic properties involving the oxidation of hydrocarbons [26] and isobutene [27–29] and as an active element in gas sensing [30–33].

A number of studies of the crystal structure have been performed using diffraction techniques, with early studies reporting a

distorted pyrochlore at ambient temperature [34,35]. Early examinations on the temperature dependence of the crystal structure suggested the presence of two phase transitions with a tetragonal phase occurring below the high temperature cubic ideal pyrochlore phase that forms above 740 °C [36]. Investigations of the polymorphism in single crystals showed that this compound exhibits the cubic pyrochlore phase, denoted γ -BSO, at temperatures higher than 680 °C [37]. Between room temperature and 90 °C the α phase was observed, and an intermediary phase, denoted β -BSO, was reported to have an acentric cubic structure [37]. The same authors observed an $\alpha \rightarrow \beta$ transition at 135 °C in polycrystalline samples, and also second harmonic generation and domains at room temperature. These results suggest that the $\alpha \rightarrow \beta$ transition is ferroic and the α phase is ferroelectric. Neutron diffraction was used to investigate the $\beta \rightarrow \gamma$ transition, which was observed at 626 °C and driven by the Bi^{3+} displacements [38,39,41]. A thorough investigation by X-ray and neutron diffraction experiments at room temperature observed the α phase being stable below 137 °C with a crystal structure belonging to the space group $Pc(C_2^2)$. The crystal structure of the α phase is very complicated, having 176 crystallographically distinct atoms. Under heating the first phase transition is associated with a change in slope of the normalized unit cell volume vs. temperature [40]. The structure of the β phase was first determined by a combination of neutron and synchrotron X-ray diffraction [41], as being cubic belonging to the $F43c(T_d^5)$ space group. On the other hand, recent synchrotron X-ray diffraction investigations associate this phase with the trigonal $P3_1(C_3^2)$ space group [42].

* Corresponding author. Tel.: +55 98 3301 8291; fax: +55 98 3301 8204.
E-mail address: paschoal@ufma.br (C.W.A. Paschoal).

Despite whether the structure is trigonal or cubic, both phases are closely related to that of the cubic pyrochlore. Comparing the polymorphs of BSO, it may be observed that the SnO_6 octahedra are fairly regular with similar Sn–O distances, whereas the Bi–O' sublattice undergoes the greatest changes [42]. The aim of this work was to investigate the temperature behavior of the Raman active phonons of the BSO pyrochlore.

2. Experimental details

Samples were synthesized by the solid-state method from stoichiometric amounts of 99.975% Bi_2O_3 and 99.9% SnO_2 (cation basis, Alfa Aesar Chemical Company, USA). Prior to each heating cycle the sample was ground with an agate mortar and pestle under acetone for 10–15 min. Samples were heated in high form alumina crucibles. Specimens were initially heated at 750°C for 12–24 h, then ground and reheated 3 times. Phase purity was ascertained, after each heating cycle, from X-ray powder diffraction data collected at ambient temperature using $\text{Cu K}\alpha$ radiation and a Rigaku Ultima III diffractometer equipped with a graphite monochromator and a scintillation detector. Equilibrium was assumed when no further changes were evident in the relative intensities of the peaks. The Jade software package (Materials Data, Inc., Livermore, CA) was used in the phase analysis.

Raman spectra were excited with 514.5 nm line radiation from an argon ion laser (Coherent Innova 70) operating at 50 mW and analyzed using a Jobin-Yvon Model T64000 Triple spectrometer in a double subtraction configuration with a spectral resolution of 2 cm^{-1} whose signal was captured with a liquid N_2 -cooled CCD detector. All spectra were obtained in the backscattering geometry. All measurements were performed using pelletized samples.

3. Results and discussion

The room temperature Raman spectrum is shown in Fig. 1. The spectrum consists of broad bands, very similar to that obtained for the α phase of $\text{Bi}_2\text{Hf}_2\text{O}_7$ [43]. At room temperature BSO crystallizes in a monoclinic structure that belongs to the space group $Pc(C_s^2)$ [44]. For this structure all 176 unique atom positions of the crystalline unit cell ($Z=32$) occupy 2a Wyckoff sites giving rise to the following distribution of Raman-active modes

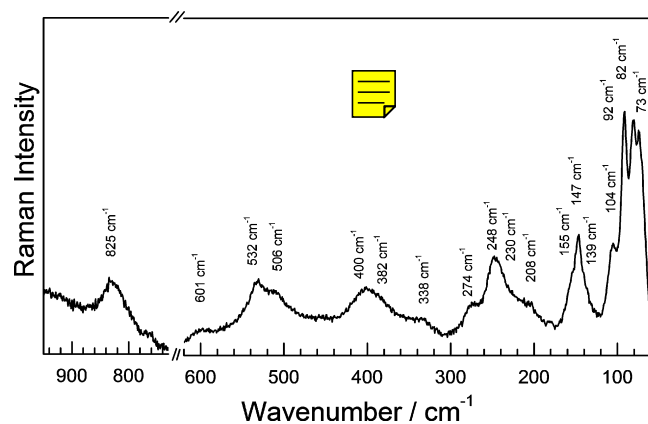


Fig. 1. Raman spectrum obtained for BSO ceramics at room temperature (corrected by the Boltzmann factor).

in terms of the irreducible representations of the $m(C_s)$ factor group.

$$\Gamma^R = 526A' \oplus 527A''$$

At ambient temperature, the factor group analysis predicts a larger number of modes in the lower symmetry space group compared to that of the ideal pyrochlore structure. The space group of the ideal cubic pyrochlore is $Fd\bar{3}m(O_h^7)$ with $Z=8$, for which the number of Raman active modes is only six, whose distribution in terms of the $m\bar{3}m(O_h)$ factor group is

$$\Gamma^R = A_{1g} \oplus E_g \oplus 4F_{2g}$$

Based on the distributions of modes of these structures, the broad Raman spectrum at room temperature could be ascribed to the convolution of the new bands originated in the symmetry lowering. A software program was used to determine the bandwidth, intensity, and line positions by fitting the peaks in the spectrum with a Lorentzian profile. The observed modes are given in Table 1. According to the literature ([45] and references therein) Raman phonons observed at wavenumbers lower than 200 cm^{-1} in pyrochlores are not due to symmetry allowed vibrations of the ideal structure. For example, bismuth-containing pyrochlores, such as

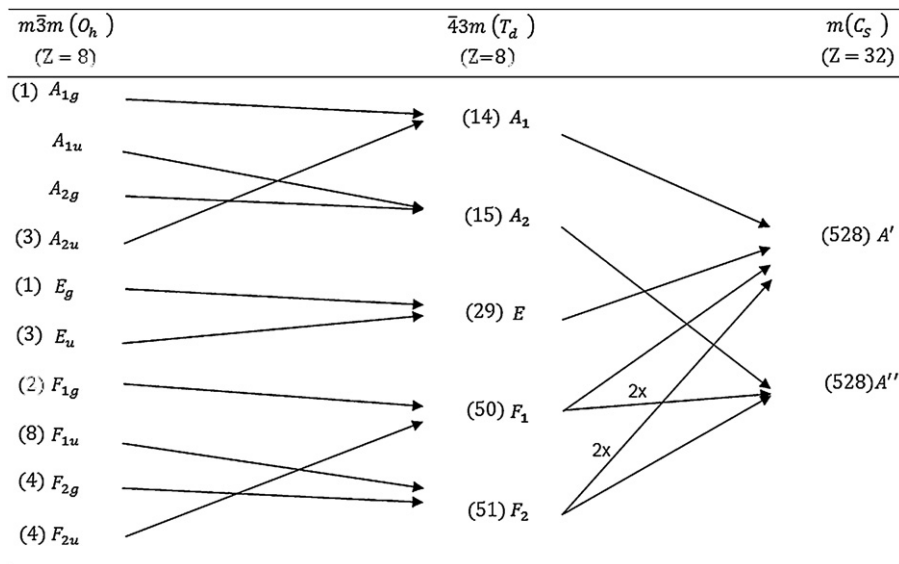


Fig. 2. Correlation diagram between the factor groups of the ideal pyrochlore structure ($m\bar{3}m(O_h)$), intermediate phase $\bar{4}3m(T_d)$ and the monoclinic room temperature structure ($m(C_s)$).

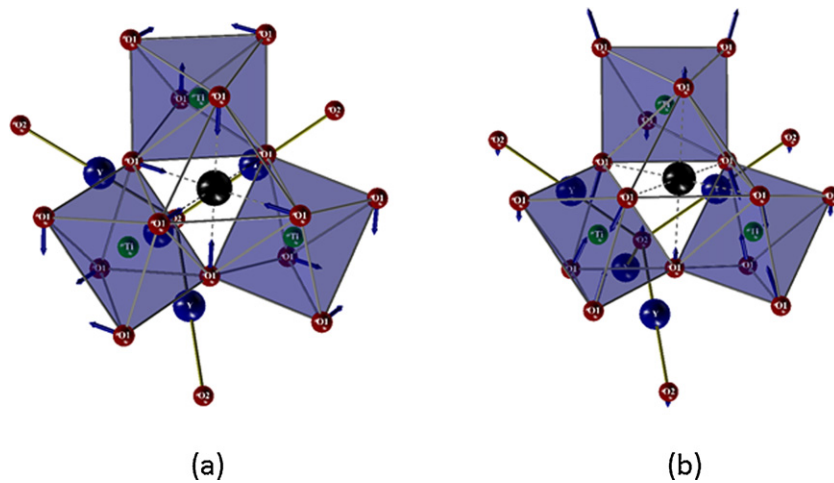


Fig. 3. The modes at 532 and 400 cm^{-1} originating from the (a) A_{1g} and (b) F_{2g} modes.

$\text{Bi}_2\text{Hf}_{2-x}\text{Ti}_{2x}\text{O}_7$ and $\text{Bi}_x\text{Y}_{2-x}\text{Ti}_2\text{O}_7$ [43] have their lowest wavenumber modes observed near 250 cm^{-1} and 226 cm^{-1} , respectively.

At room temperature several modes were observed at wavenumbers lower than 200 cm^{-1} in the BSO. These modes are due to infrared active and silent modes that are not permitted in the Raman spectra of the ideal pyrochlore structure, but become active in the $Pc(C_2^2)$ structure, as shown in the correlation diagram between the irreducible representations of both points groups (Fig. 2). All phonons of the ideal pyrochlore structure are permitted in the polar monoclinic low symmetry phase. Comparing the observed phonons to those recorded using infrared spectroscopy in other pyrochlores, we can identify the (F_{1u}) modes of the ideal pyrochlore structure (O'–Bi–O' bending, O–Bi–O bending and Bi– SnO_6 stretching) [46–48].

In the intermediate region of the spectrum, between 200 and 400 cm^{-1} , seven modes were observed. Some of the modes were assigned by comparison to infrared active modes resulting from the symmetry lowering, which were classified according to the IR

data of related pyrochlores [46–48]. In this region we assigned the modes observed at 274 and 382 cm^{-1} as being due to the O–Sn–O bending and Bi–O stretching. There are two modes in this region which originated from the Raman active modes of the ideal pyrochlore structure. Similar to other pyrochlores, the (F_{2g}) is observed at lower wavenumbers than (E_g) mode in this region, thus we have assigned the 230 cm^{-1} and 248 cm^{-1} modes as originating from the (F_{2g}) and (E_g) modes, respectively.

Four bands were observed in the region with wavenumbers higher than 400 cm^{-1} . The modes at 532 cm^{-1} and 400 cm^{-1} originate from the (A_{1g}) and (F_{2g}) modes, respectively. These modes are usually classified as due to the O–Sn–O bending and the Sn–O stretching, respectively [49–56]. Recently, this mode was discussed in terms of an alternative visualization model considering a symmetric breathing motion of the O1 octahedron toward the vacant 8a site at (1/8, 1/8, 1/8) [58,59]. Using the force constants reported by Gupta et al. in Ref. [57], the eigenvectors of the normal modes of an ideal pyrochlore structure were calculated confirming the previous

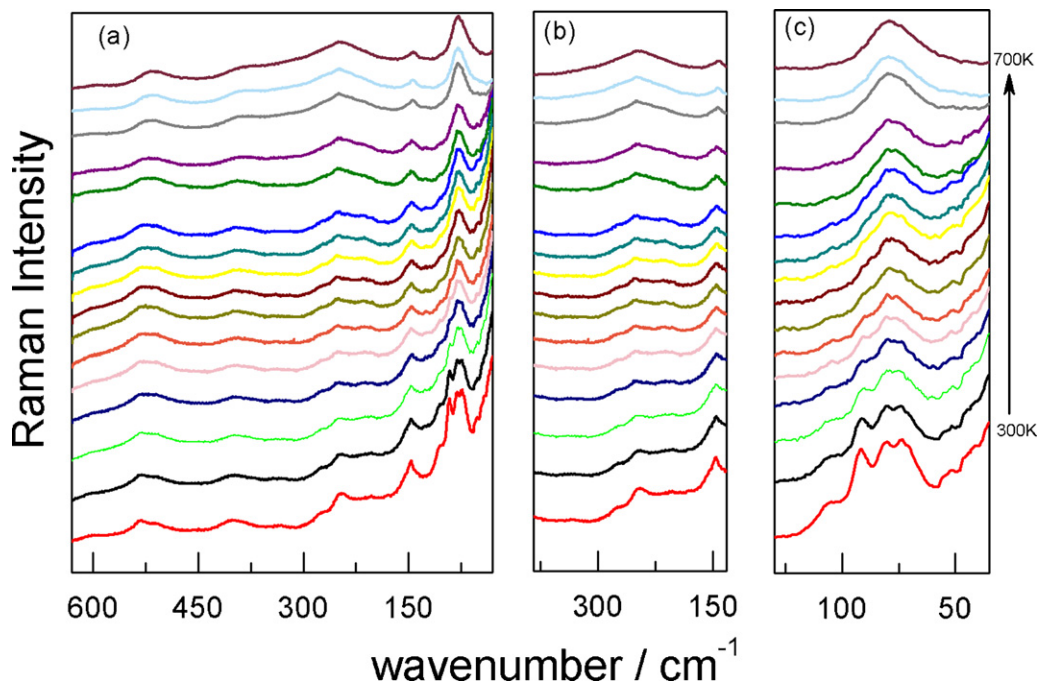


Fig. 4. Temperature dependent Raman spectra obtained for BSO.

Table 1
Observed Raman active phonons at room temperature.

Wavenumber (cm^{-1})	Assignment
73 m	O'—Bi—O' bending (F_{1u})
82 m	A_{2u}
92 m	
104 w	A_{2u}
139 w	O—Bi—O bending (F_{1u})
147 s	O—Bi—O bending (F_{1u})
155 sh	
193 w	
208 w	Bi— SnO_6 stretching (F_{1u})
230 sh	
248 s	(F_{2g})
338 w	(E_g)
274 m	O—Sn—O bending (F_{1u})
382 m	Bi—O stretching (F_{1u})
400 s	O motion in SnO_6 polyhedra (F_{2g})
506 s	Bi—O' stretching (F_{1u})
532 s	O'—vacancy stretching (A_{1g})
600 w	
825 b	Overtone or combination

Abbreviations: m, a mode with medium intensity; sh, shoulder; s, strong; w, weak; b, broad.

model, as shown in Fig. 3(a). The (F_{2g}) mode was usually associated to a Sn—O stretching, however a careful analysis of the calculated vibrations in the ideal pyrochlore structure shows that the oxygen displacement is not exactly along the Sn—O bond, except for the one that is related to the Bi motion and has lower wavenumber. As a consequence, we have classified the (F_{2g}) mode as being due to the O1 motion in SnO_6 polyhedra, as shown in Fig. 3(b). Finally, a weak band was observed at 825 cm^{-1} , which is similar to that observed by Arenas et al. [45] near 800 cm^{-1} . This mode was not classified for other pyrochlores that exhibit the ideal structure, being attributed to the overtone or combination modes [58].

Fig. 4 shows the temperature-dependent Raman spectra of BSO at temperatures up to 700 K. The general feature of the temperature evolution of the spectra follows a normal trend with the Raman intensity of the modes lowering with increasing temperature. The more apparent change in the spectra occurs at modes near 100 cm^{-1} , where we see only a broad mode at high temperatures. Fig. 5 shows the temperature dependence of the mode positions. We see that several modes exhibit a change in wavenumber near the α – β structural phase transition that BSO undergoes

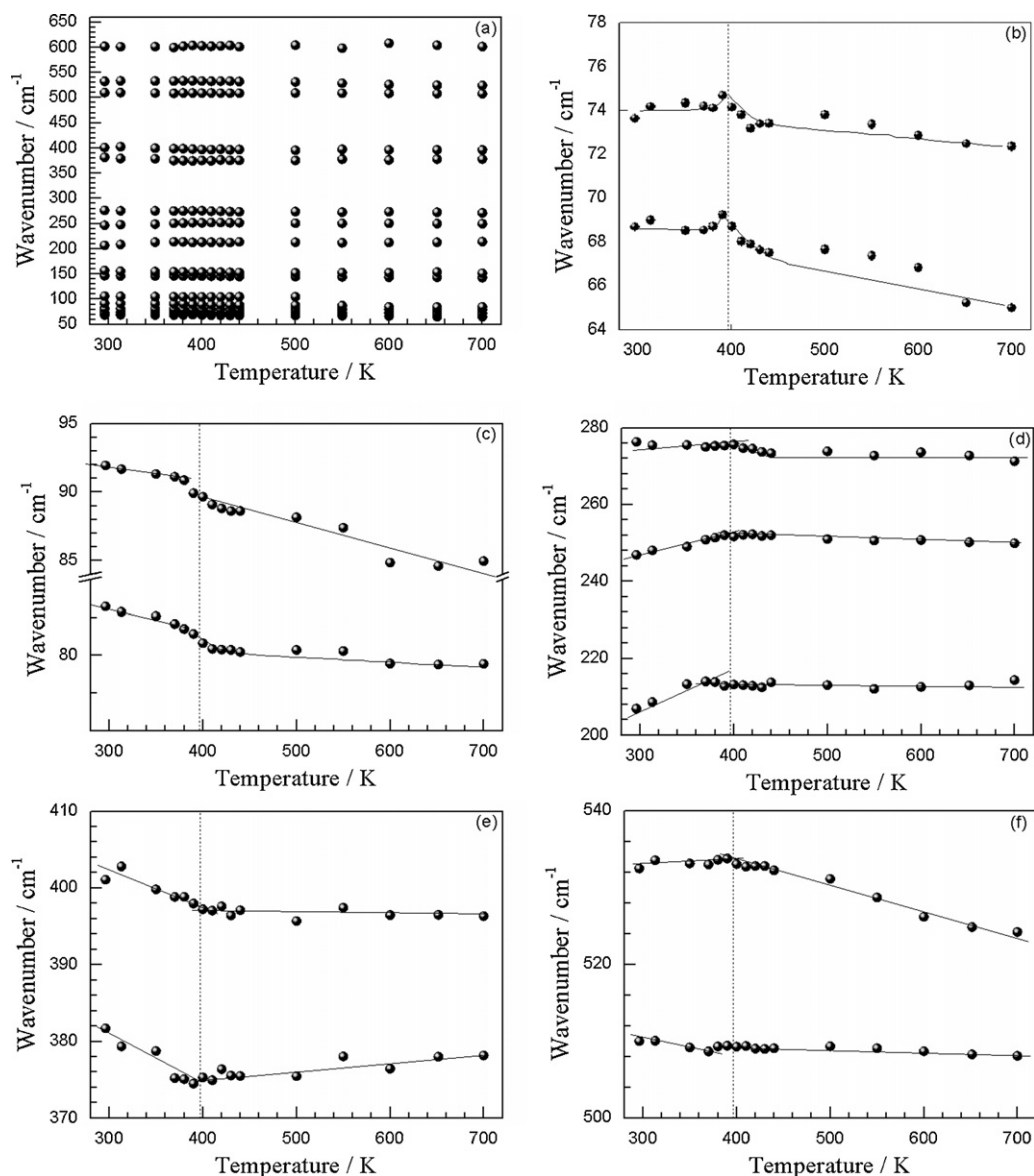


Fig. 5. Temperature dependence of the position of the Raman modes observed for BSO. (a) All modes. (b–f) Individual behavior for representative modes. The solid lines are guide for the eyes.

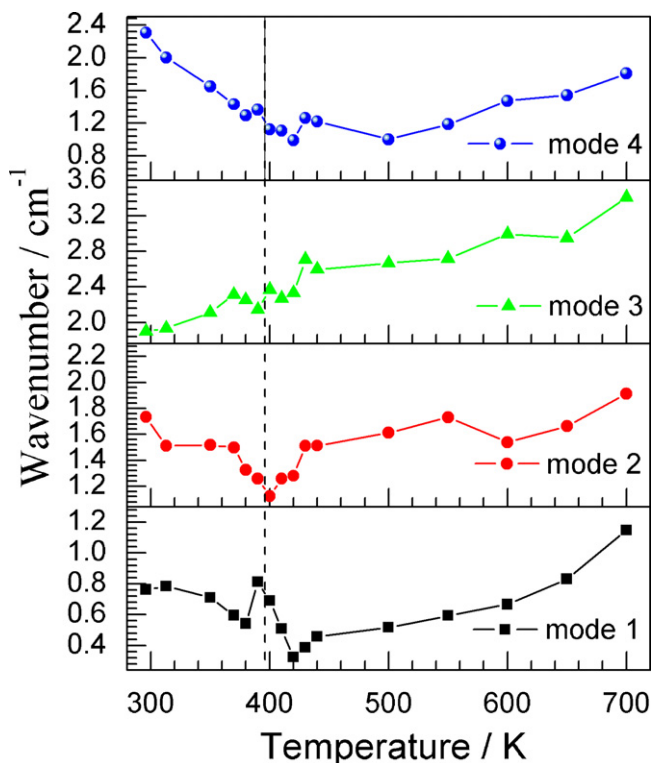


Fig. 6. Temperature dependence of the relative intensity of the modes near 100 cm^{-1} . All the intensities were calculated relative to the intensity of the mode near 140 cm^{-1} . The designated modes 1–4 indicate the modes in increasing wavenumber order as shown in Fig. 1.

near 127°C . This effect being very subtle in the spectra shown in Fig. 4, but is more apparent in the positions of the modes shown in Fig. 5. This trend is also observed in the temperature dependence of the relative intensity of several modes, as shown in Fig. 6. A similar trend was observed with $\text{Bi}_2\text{Hf}_2\text{O}_7$ in the Henderson et al. work [43], where broad bands were observed at high temperatures. In the β -phase $\text{Bi}_2\text{Hf}_2\text{O}_7$ crystallizes in a face-centered cubic cell, which is possibly a double cubic unit cell belonging to the space group $F43c(T_d^5)$, similar to that reported for the β -phase BSO by Kennedy et al. [41]. In order to understand the absence of significant changes in the spectra when the $\alpha \rightarrow \beta$ phase transition occurs, we consider the correlation between the more symmetric pyrochlore structure and this structure which is given in Fig. 2. We can see that the transition of the ideal pyrochlore to $F43c(T_d^5)$ phase permits several modes whose selection rules were inhibited in the ideal phase. When the $\alpha \rightarrow \beta$ transition occurs, the superposition of modes results in minor changes in the spectra. Although the structure of BSO at room temperature is monoclinic and several degenerate modes are broken through the $\alpha \rightarrow \beta$ transition, the monoclinic distortion is low and this splitting of all the allowed modes is unable to be fully resolved at room temperature.

4. Conclusions

The Raman spectrum of BSO was measured at room temperature and 19 modes were observed. The symmetries of these modes were discussed using the basis of well-established modes for other related pyrochlore-based compounds. The temperature dependence of the Raman active phonons was investigated, displaying the $\alpha \rightarrow \beta$ structural phase transition in the temperature behavior of the mode centers and in the relative intensities. This study illustrates the utility of Raman spectroscopy in the investigation of phase transitions of complex oxides.

Acknowledgments

The Brazilian authors acknowledge the financial support from CNPq, CAPES, FAPEMA and FAPEMIG funding agencies. MWL acknowledges financial support from Research Corporation and UNF for the Munoz Professorship.

References

- [1] M.A. Subramanian, G. Aravamudan, G.V.S. Rao, *Prog. Solid State Chem.* 15 (1983) 55.
- [2] T.A. Vanderah, I. Levin, M.W. Lufaso, *Eur. J. Inorg. Chem.* 14 (2005) 2895.
- [3] G. Jeanne, G. Desgardin, G. Allais, B. Raveau, *J. Solid State Chem.* 15 (1975) 193.
- [4] D. Bernard, J. Pannetier, J. Lucas, *Ferroelectrics* 21 (1978) 429.
- [5] C.A. Randall, et al., *Am. Ceram. Soc. Bull.* 82 (2003) 9101.
- [6] R.J. Cava, W.F. Peck, J.J. Krajewski, *J. Appl. Phys.* 78 (1995) 7231.
- [7] S.J. Korf, H.J.A. Koopmans, B.C. Lippens, A.J. Burggraaf, P.J. Gellings, *J. Chem. Soc. Faraday Trans. 1* 83 (1987) 1485.
- [8] S. Yonezawa, Y. Muraoka, Y. Matsushita, Z. Hiroi, *J. Phys. Soc. Jpn.* 73 (2004) 819.
- [9] E. Beck, A. Ehmann, B. Krutzsch, S. Kemmlersack, H.R. Khan, C.J. Raub, *J. Less-Common Met.* 147 (1989) L17.
- [10] G.M. Kurthy, W. Wischert, R. Kiemel, S. Kemmlersack, R. Gross, R.P. Huebener, *J. Solid State Chem.* 79 (1989) 34.
- [11] L.Q. Li, B.J. Kennedy, *Chem. Mater.* 15 (2003) 4060.
- [12] J.B. Goodenough, R.N. Castellano, *J. Solid State Chem.* 44 (1982) 108.
- [13] S.J. Korf, H.J.A. Koopmans, B.C. Lippens, A.J. Burggraaf, P.J. Gellings, *J. Chem. Soc. Faraday Trans. 1* 83 (1987) 1485.
- [14] R.A. Mccauley, F.A. Hummel, *J. Lumin.* 6 (1973) 105.
- [15] R.G. Dosch, T.J. Headley, P. Hlava, *J. Am. Ceram. Soc.* 67 (1984) 354.
- [16] A.J. Burggraaf, T. Vandijk, M.J. Verkerk, *Solid State Ionics* 5 (1981) 519.
- [17] S. Kramer, M. Spears, H.L. Tuller, *Solid State Ionics* 72 (1994) 59.
- [18] C. Heremans, B.J. Wuensch, J.K. Stalick, E. Prince, *J. Solid State Chem.* 117 (1995) 108.
- [19] O. Porat, C. Heremans, H.L. Tuller, *J. Am. Ceram. Soc.* 80 (1997) 2278.
- [20] R. Vassen, X.Q. Cao, F. Tietz, D. Basu, D. Stover, *J. Am. Ceram. Soc.* 83 (2000) 2023.
- [21] X.Q. Cao, R. Vassen, W. Jungen, S. Schwartz, F. Tietz, D. Stover, *J. Am. Ceram. Soc.* 84 (2001) 2086.
- [22] J. Wu, X.Z. Wei, N.P. Padture, P.G. Klemens, M. Gell, E. Garcia, P. Miranzo, M.I. Osendi, *J. Am. Ceram. Soc.* 85 (2002) 3031.
- [23] D. Huiling, Y. Xi, *J. Phys. Chem. Solids* 63 (2002) 2123.
- [24] W.R. Cook, H. Jaffe, *Phys. Rev.* 89 (1953) 1297.
- [25] B. Li, J. Zhang, *J. Am. Ceram. Soc.* 72 (1989) 2377.
- [26] C.A. Mims, A.J. Jacobson, R.B. Hall, J.T. Lewandowski, *J. Catal.* 153 (1995) 197.
- [27] L. Moens, P. Ruiz, B. Delmon, M. Devillers, *Appl. Catal. A: Gen.* 171 (1998) 131.
- [28] L. Moens, P. Ruiz, B. Delmon, M. Devillers, *Appl. Catal. A: Gen.* 180 (1999) 299.
- [29] L. Moens, P. Ruiz, B. Delmon, M. Devillers, *Appl. Catal. A: Gen.* 249 (2003) 365.
- [30] G.S.V. Coles, S.E. Bond, G. Williams, *J. Mater. Chem.* 4 (1994) 23.
- [31] G.S. Devi, S.V. Manorama, V.J. Rao, *J. Electrochem. Soc.* 145 (1998) 1039.
- [32] G.S. Devi, S.V. Manorama, V.J. Rao, *Sens. Actuators B: Chem.* 56 (1999) 98.
- [33] T.D. Malinovsky, A.I. Aparnev, Y.P. Egorov, Y.M. Yukhin, *Russ. J. Appl. Chem.* 74 (2001) 1864.
- [34] R.S. Roth, *J. Res. Natl. Bur. Stand.* 56 (1956) 17.
- [35] F. Brisse, O. Knop, *Can. J. Chem.* 46 (1968) 859.
- [36] G. Vetter, F. Queyroux, J.C. Gilles, *Mater. Res. Bull.* 13 (1978) 859.
- [37] R.D. Shannon, J.D. Bierlein, J.L. Gillson, G.A. Jones, A.W. Sleight, *J. Phys. Chem. Solids* 41 (1980) 117.
- [38] V. Kahlenberg, T. Zeiske, *Z. Kristallogr.* 212 (1997) 297.
- [39] R.H. Jones, K.S. Knight, *J. Chem. Soc. Dalton* 15 (1997) 2551.
- [40] I.R. Evans, J.A.K. Howard, J.S.O. Evans, *J. Mater. Chem.* 2098 (2003) 13.
- [41] B.J. Kennedy, Ismunandar, M.M. Elcombe, *Mater. Sci. Forum* 278 (1998) 762.
- [42] A. Salamat, A.L. Hector, P.F. McMillan, C. Ritter, *Inorg. Chem.* 50 (2011) 11905.
- [43] S.J. Henderson, O. Shebanova, A.L. Hector, P.F. McMillan, M.T. Weller, *Chem. Mater.* 19 (2007) 1712.
- [44] I.R. Evans, J.A.K. Howard, J.S.O. Evans, *J. Mater. Chem.* 13 (2003) 2098.
- [45] D.J. Arenas, L.V. Gasparov, W. Qiu, J.C. Nino, C.H. Patterson, D.B. Tanner, *Phys. Rev. B* 82 (2010), Art. 214302.
- [46] M.H. Chen, D.B. Tanner, J.C. Nino, *Phys. Rev. B* 72 (2005), Art. 54303.
- [47] H. Wang, S.R. Foltyn, Q.X. Jia, P.N. Arendt, X. Zhang, *J. Appl. Phys.* 100 (2006), Art. 053904.
- [48] M. Fischer, T. Malcherek, U. Bismayer, P. Blaha, K. Schwarz, *Phys. Rev. B* 78 (2008), Art. 014108.
- [49] S. Brown, H.C. Gupta, J.A. Alonso, M.J. Martinez-Lopez, *Phys. Rev. B* 69 (2004), Art. 054434.
- [50] H.C. Gupta, S. Brown, N. Rani, V.B. Gohel, *Int. J. Inorg. Mater.* 3 (2001) 983.
- [51] N.T. Vandenberg, E. Husson, H. Brusset, *Spectrochim. Acta A* 37 (1981) 113.
- [52] C.S. Knee, J. Holmlund, J. Andreasson, M. Kall, S.G. Eriksson, L. Borjesson, *Phys. Rev. B* 71 (2005), Art. 214518.
- [53] M. Maczka, M.L. Sanjuan, A.F. Fuentes, K. Hermanowicz, J. Hanuza, *Phys. Rev. B* 78 (2008), Art. 134420.

- [54] F. Rosi, V. Manuali, C. Miliani, B.G. Brunetti, A. Sgamellotti, T. Grygar, D. Hradil, J. Raman Spectrosc. 40 (2009) 107.
- [55] A. Garbout, A. Rubbens, R.N. Vannier, S. Bouattourl, A.W. Kolsil, J. Raman Spectrosc. 39 (2008) 1469.
- [56] M. Maczka, J. Hanuza, K. Hermanowicz, A.F. Fuentes, K. Matsuhira, Z. Hiroi, J. Raman Spectrosc. 39 (2008) 537.
- [57] H.C. Gupta, S. Brown, N. Rani, V.B. Gohel, J. Raman Spectrosc. 32 (2001) 41.
- [58] M. Maczka, M.L. Sanjuán, A.F. Fuentes, L. Macalik, J. Hanuza, K. Matsuhira, Z. Hiroi, Phys. Rev. B 79 (2009) 214437.
- [59] T. Hasegawa, Y. Takasu, N. Ogita, M. Udagawa, J.I. Yamaura, Y. Nagao, Z. Hiroi, Phys. Rev. B 77 (2008) 064303.